Size-dependent electric voltage controlled magnetic anisotropy in multiferroic heterostructures: Interface-charge and strain comediated magnetoelectric coupling

Jia-Mian Hu, Ce-Wen Nan, and Long-Qing Chen

Size dependent electric voltage-controlled magnetic anisotropy in multiferroic

heterostructures: Interface-charge and strain co-mediated magnetoelectric coupling

Jia-Mian Hu,[1,2] Ce-Wen Nan,[1*] and Long-Qing Chen[2]

[1]*Department of Materials Science and Engineering, and State Key Lab of New Ceramics and Fine Processing, Tsinghua University, Beijing 100084, China*

[2]*Department of Materials Science and Engineering, Pennsylvania State University, University Park, Pennsylvania 16802-5005*

Abstract

We present a phenomenological scheme to study the size-dependent electric voltage-controlled magnetic anisotropy in ferromagnetic (FM)/ferroelectric (FE) heterostructures. The FM layers are either metallic Fe(001), Ni(001), Co(0001), or half-metallic (La, Sr)MnO$_3$ films. Two magnetoelectric mechanisms, i.e., interface-charge and strain-mediated couplings, are considered. We show that the interface-charge mediated coupling is the main mechanism for the magnetoelectic coupling when the FM film thickness is below a certain transition thickness d_{tr} while the strain-mediated coupling dominates above d_{tr}.

Artificial multiferroic heterostructures of ferroelectric (FE) and ferromagnetic (FM) layers are of increasing interest due to the coupling between the magnetic and electric polarizations.[1–3] Of particular interest in the multiferroic heterostructures, electric voltage, rather than the usual current or magnetic field, can be directly used to control the magnetic anisotropy or magnetization direction via magnetoelectric (ME) coupling,[1–5] which offers promising applications for novel spintronic or ME devices with much lower power consumption and higher speed. Examples include voltage-driven magnetic random access memories,[6–8] logic circuits,[9] and microwave devices.[10,11] Much effort has been devoted to achieve robust *room-temperature* ME coupling by virtue of such FE/FM heterostructures either through a strain-induced ME effect across an interface,[4,12–18] or interface-charges driven ME effect,[19–23] or magnetic exchange bias.[24–29] As demonstrated recently in the multiferroic heterostructures, a remarkable electric-voltage control of magnetic behavior of the magnetic nanostructures at *room temperature* can be achieved by a strain-induced ME coupling, i.e., an external voltage in the ferroelectric layer causing a strain change across the interface and then altering the magnetic anisotropy of the magnetic layer via magnetoelastic coupling. For example, a butterfly-shaped magnetization (M)–electric field (E) loop at room temperature has recently been observed in a multiferroic FM/FE heterostructure with a $La_{0.7}Sr_{0.3}MnO_3$ (LSMO, 20-50 nm) thin film grown on $Pb(Mg_{1/3}Nb_{2/3})_{0.72}Ti_{0.28}O_3$ (PMN-PT), which tracks the butterfly-shaped strain–E loop of PMN-PT, demonstrating a strain-induced ME coupling across the LSMO/PMN-PT interface.[12] However, in a multiferroic $PbZr_{0.2}Ti_{0.8}O_3$ (PZT, 250 nm)/LSMO (4 nm)/$SrTiO_3$ (001) heterostructure,[19] a totally

different square-shaped *M-E* hysteric loop has been observed at 100 K. Although a larger

piezostrain could be expected in such a reverse FE/FM/substrate structure, further tests

using x-ray absorption near edge spectroscopy[20] explicitly illustrated an interface-charge

driven ME coupling, i.e., a direct voltage-induced modification of the magnetocrystalline

anisotropy through a change in interfacial spin configuration.[21-23] This discrepancy thus

raises important questions: why do the two heterostructures behave differently, or do these

two different ME coupling mechanisms operate independently? In this work, we

demonstrate these coupling mechanisms could coexist and tend to interact with each other at

the interfaces. Specifically, the interface-charge mediated ME coupling exerts major

influences for ultrathin FM films while the strain-mediated ME coupling operates at larger

thickness, leading to a size dependent electric-voltage control of magnetic anisotropy.

In this article we present a phenomenological approach to investigate such size effect

of the ME coupling in the multiferroic FM/FE heterostructure, where the influences of two

mechanisms for the ME coupling, i.e., the interface-charge and strain-mediated coupling,

are addressed. For illustration, we consider different FM films including either metallic

Fe(001), Ni(001), Co(0001), or half-metallic (001)-oriented LSMO films, grown on a FE

layer such as $BaTiO_3$(001). The results show that there is a transition thickness d_{tr} for the

FM films, i.e., in the FM/FE heterostructures with a thin FM film below d_{tr}, the

interface-charge mediated coupling plays a major part, while the strain-mediated ME

coupling predominates when the FM film thickness is larger than d_{tr}.

Consider a multiferroic structure with a FM thin film grown on a FE layer, and an

electric voltage V applied longitudinally across the FE layer. Then the total magnetic anisotropy energy $F_{tot}(V)$ of the FM film in a single-domain state is,[7,8,18]

$$F_{tot}(V) = F_{mc} + F_{shape} + F_{me}(V) + F_S(V),$$ (1)

where F_{mc} is the magnetocrystalline anisotropy, F_{shape} the shape anisotropy, F_{me} the magnetoelastic anisotropy, and F_S surface anisotropy, The strain-induced coupling across the interface and the interface-charge driven coupling are mainly related to the magnetoelastic anisotropy F_{me} and the surface anisotropy F_S, respectively, where F_S can be expressed as,[22,30]

$$F_{surf} = -\frac{2K_s + \Delta K_s(V)}{d} m_3^2,$$ (2)

here m_3 refers to the direction cosine; K_s and $\Delta K_s(V)$ denote the surface anisotropy energy and its change under external electric voltage V; and d is the thickness of the FM film. Any changes in the interface charges would alter the surface anisotropy, and hence the magnetization state.

For simplicity, the effective magnetic anisotropy field H_{eff}[10,11,31] is used to investigate the voltage-controlled magnetic anisotropy (H_{eff} usually shares similar variation trend with the magnetic coercive field H_c[32]). Thus the out-of-plane effective anisotropy field, i.e., H_{eff}^{OP}, can be determined by

$$H_{eff}^{OP} = -\frac{1}{\mu_0 M_s} \frac{\partial F_{tot}}{\partial m_3}\Bigg|_{m_3=1},$$ (3)

where μ_0 and M_s are the vacuum permeability and the saturation magnetization, respectively. Combination of Eq. (3) with Eq. (1) yields under zero voltage bias

$$H_{eff}^{OP} = \frac{2K_1}{M_s} - \mu_0 M_s + \frac{2\left[B_1\left(1+\dfrac{2c_{12}}{c_{11}}\right)\varepsilon_0\right]}{M_s} + \frac{4K_s}{dM_s},$$

(4a)

for cubic (001)-oriented FM films, and

$$H_{eff}^{OP} = \frac{2K_1}{M_s} - \mu_0 M_s - \frac{2B_4^2}{c_{44}M_s} + \frac{2\left(B_1 + 2B_3 - \dfrac{2B_2 c_{13}}{c_{33}}\right)\varepsilon_0}{M_s} + \frac{4K_s}{dM_s}$$

(4b)

for hexagonal (0001) films. K_1 and B_i (i=1,2,3,4) denote the magnetocrystalline and magnetoelastic constants, respectively; c_{ij} and ε_0 are the elastic stiffness constants and the residual strain in the FM films, respectively. H_{eff}^{OP} can be experimentally obtained from an out-of-plane magnetic hysteresis loop.[33] An out-of-plane magnetic easy axis (or spontaneous magnetization) is preferred for $H_{eff}^{OP} > 0$, and a change in the sign of H_{eff}^{OP} from positive to negative would indicate an easy axis reorientation[18] from an out-of-plane to an in-plane direction, or vice versa. Such a reorientation depending on the film thickness has been reported in FM thin films.[30,34,35] For example, in a Ni/Cu(001) heterostructure,[34] the easy axis of the magnetization switched abruptly from initial in-plane to out-of-plane at a critical thickness d_{cr} of about 10.5 monolayers (ML) (i.e., ~1.6 nm). The critical thickness d_{cr} for such an easy axis reorientation can be estimated from $H_{eff}^{OP} = 0$, i.e., $d_{cr} = 2K_s \Big/ \left[\frac{1}{2}\mu_0 M_s^2 - K_1 - B_1\left(1+2c_{12}/c_{11}\right)\varepsilon_0\right]$. By using the known material parameters,[36] and the residual strain ε_0 of 2.5% arising from the in-plane lattice mismatch between Ni film and Cu(001) substrate,[34] one can obtain d_{cr} of about 1.73 nm for the Ni film, well consistent with the experimental value (~1.6 nm), demonstrating that this effective anisotropy field approach is valid.

Now let us return to the change in the magnetic anisotropy under the application of longitudinal electric voltages to the bilayer structure, i.e., ΔH_{eff}^{OP} [$= H_{eff}^{OP}(V)/H_{eff}^{OP}(0)-1$], which can be obtained as,

$$\Delta H_{eff}^{OP} = \frac{2\left[B_1\left(1+\frac{2c_{12}}{c_{11}}\right)\varepsilon_p(V)+\frac{\Delta K_s(V)}{d}\right]}{M_s}\bigg/H_{eff}^{OP} \tag{5a}$$

for cubic (001) FM films, and,

$$\Delta H_{eff}^{OP} = \frac{2\left[\left(B_1+2B_3-\frac{2B_2c_{13}}{c_{33}}\right)\varepsilon_p(V)+\frac{\Delta K_s(V)}{d}\right]}{M_s}\bigg/H_{eff}^{OP} \tag{5b}$$

for hexagonal (0001) films. $\varepsilon_p(V)$ denotes the piezostrain under external voltage. The two terms in the square brackets on the right hand side of Eq. (5) describe the contributions from the strain and the interface-charge mediated ME coupling. Thus these two mechanisms coexist in the FM/FE bilayer structure and compete with each other.

For illustration, the calculations are performed for the FM films by using the known material parameters,[36] and a common BaTiO$_3$ (BTO) film with a thickness of about 100 nm grown on (001) SrTiO$_3$ substrate[41] is chosen as the FE layer, with SrRuO$_3$ as a bottom electrode. The butterfly-shaped curve of piezostrain $\varepsilon_p(V)$ shown in Fig. 1(a) was measured in the BTO film using a piezoelectric force microscope. For the metallic Fe(001) films, the hysteresis-like change in $\Delta K_s(V)$ [Fig. 1(b)] is directly obtained from the experimental measurements of voltage-controlled magnetic anisotropy in ultrathin Fe atomic layers.[22] However, no results on the voltage-induced magnetic anisotropy are now available for the metallic Ni(001) and Co(0001) films. For the sake of simplicity, the same $\Delta K_s(V)$ is tentatively used for the Ni(001) and Co(0001) films herein, though $\Delta K_s(V)$

could be different in these three transition-metal films and support from both experiments and *ab inito* calculations are awaited. Actually, recent density functional calculations[42] showed that ultrathin Ni and Co films exhibited quite similar voltage-induced surface ME coefficients to Fe, i.e., 2.9×10^{-14} G cm^2/V for a 15-ML Fe(001) film with perpendicular [001] magnetization, 3.0×10^{-14} G cm^2/V for 9-ML Ni(001) with in-plane [100] magnetization, and 1.7×10^{-14} G cm^2/V for 9-ML Co(0001) film with [001] magnetization.

As the first example, the electric voltage-induced changes in H_{eff}^{OP} for the (001) Fe/BTO thin-film heterostructure are shown in Fig. 2(a). It shows distinct size-dependent characteristics of the voltage-controlled out-of-plane effective anisotropy field, i.e., ΔH_{eff}^{OP}, demonstrating the coexistence of both the interface-charge and strain mediated ME coupling in the heterostructure. A transition thickness d_{tr} for the two interacting ME coupling mechanisms can be estimated to be about 0.5 nm (about one-unit cell thickness) as the contributions from the two mechanisms become equal from Eq. (5). Thus, when the Fe film thickness is smaller than d_{tr} (e.g., 0.2 nm), the ΔH_{eff}^{OP}-voltage curve tends to mimic the voltage-induced surface anisotropy change behavior, i.e., a hysteresis-like loop [see Fig. 2(a)], indicating that the interface-charge mediated ME coupling could play a major part. However, the ΔH_{eff}^{OP}-voltage loops become butterfly-shaped as the film thickness exceeds d_{tr}, presenting a dominant strain-mediated ME effect. An external voltage leads to larger changes in ΔH_{eff}^{OP} in Fe films with smaller thickness (i.e., below d_{tr}), as compared to those with thickness larger than d_{tr}. Such larger ΔH_{eff}^{OP} can in principle allow a more dramatic voltage-induced magnetic anisotropy change based on a dominative interface-charge ME

coupling in the reduced thickness scale. Moreover, the maximal value of ΔH_{eff}^{OP} emerges at

d=0.3 nm to be about 20% under the action of negative voltages, which could be attributed

to the enhanced sensitivity of ΔH_{eff}^{OP} to both the external voltage and the residual strain

when approaching the transition thickness d_{tr}, as illustrated in Fig. 2(b). Furthermore, it can

be seen that the ΔH_{eff}^{OP}-voltage loop reverses as the film thickness increases from 0.3 nm to

1 nm, owing to a sign change of H_{eff}^{OP} at a critical thickness d_{cr} of about 0.39 nm (not

shown here) where the magnetic easy axis of the Fe film switches from an out-of-plane to

an in-plane direction.

   In comparison with the Fe(001) film, the Ni(001) film presents different behavior, as

shown in Figure 3(a) for ΔH_{eff}^{OP} in the (001) Ni/BTO bilayer structure. A butterfly-shaped

ΔH_{eff}^{OP}-voltage curve is clearly shown even when the film thickness is reduced to 0.15 nm

[see the inset of Fig. 3(a)], demonstrating the dominant influence of strain-mediated ME

coupling in the (001) Ni/BTO heterostructure. Similarly to the (001) Fe/BTO case, the

ΔH_{eff}^{OP}-voltage curves reverse as the film thickness d exceeds the critical d_{cr} of about 1.76

nm (at ε_0=2.5%[34]) and exhibit enhanced ΔH_{eff}^{OP} in the vicinity of d_{cr} where H_{eff}^{OP} changes

significantly. The (0001) Co/BTO structure presents also quite similar behavior [Fig. 3(b)],

i.e., butterfly-shaped ΔH_{eff}^{OP}-voltage behavior, demonstrating the dominant influence of

strain-mediated ME coupling. Therefore, a significant interface-charge mediated ME

coupling may be difficult to be observed in such (001) Ni/BTO and (0001) Co/BTO bilayers

wherein a robust strain-mediated ME coupling is always present. Meanwhile, the

strain-induced ΔH_{eff}^{OP} in these two cases are much larger than that in the (001) Fe/BTO

structure due to their larger magnetoelastic coupling coefficients.[36] Moreover, it should be noted that these butterfly-shaped ΔH_{eff}^{OP}-voltage loops in the (001) Ni/ and (0001) Co/BTO bilayers exhibit opposite trends. This is due to the opposite signs of H_{eff}^{OP} and different K_s[36] observed in the Ni(001) and Co(0001) films.

Now turn to an even more interesting FM/FE heterostructure consisting of FM half-metal like LSMO. LSMO is used due to its high sensitivity of a strongly correlated magnetic state to the charge carriers.[19,20] In half-metals, the screening interface-charges are usually 100% spin-polarized, which in principle allows stronger ME coupling[43,44] as compared to the partial spontaneous spin polarization in FM metals such as Fe, Ni, and Co. For example, a universal surface ME constant of about 6.44×10^{-14} G cm^2/V was derived for all FM half-metals,[44] which is about two to three times higher than that for FM metals as mentioned above. Thus a larger voltage-induced surface anisotropy change is assumed for the half-metallic LSMO(001) films, as shown in Fig. 4(a). The sharp changes of ΔK_s in the vicinity of the FE coercive field can be related to the two distinct states for the spin-polarized interface charges resulting from the FE polarization reversal, i.e., the accumulation and the depletion state, respectively, as observed in a recent experiment.[19,20] Similarly to the case of the (001) Fe/BTO structure, the (001) LSMO/BTO heterostructure presents either hysteresis-like or butterfly-shaped ΔH_{eff}^{OP}-voltage loops at room temperature [Fig. 4(b)], depending on the thickness of the LSMO films, exhibiting the interface-charge and strain co-mediated ME coupling. However, the room-temperature transition thickness d_{tr} in the (001) LSMO/BTO case is significantly larger than that in the (001) Fe/BTO case, i.e.,

about 4.2 nm, owing to an enhanced ME coupling and thus the larger voltage-induced surface anisotropy change ΔK_s as discussed above. Furthermore, it can be seen that change in ΔH_{eff}^{OP} is greater in LSMO films with thickness above d_{tr} than that in LSMO thin films, indicating the voltage-controlled magnetic anisotropy change may be more significant in the thick LSMO(001) films where the strain-mediated ME coupling dominates, as observed in recent experiments.[12,19,20] The ΔH_{eff}^{OP}-voltage curves of the LSMO/BTO structure at low temperature present a similar size-dependent behavior [Fig. 4(c)] to its room temperature case. However, it can be expected that the interface-charge mediated ME effect would become more remarkable at low temperature in comparison with the suppressed strain-mediated ME coupling due to reduced piezoelectric strains, which can further lead to a larger transition thickness d_{tr}, demonstrating a major influence of the interface-charge mediated ME coupling within a wider thickness range.

In conclusion, a simple phenomenological model is able to describe the size dependent electric voltage-controlled magnetic anisotropy in multiferroic heterostructures. The interface-charge and strain mediated coupling coexist and interact with each other in bilayer structures. A transition thickness d_{tr} is defined to describe the competition between these two coupling mechanisms, below which the influence of the interface-charge mediated ME coupling would outweigh that of the strain-mediated ME coupling. The calculations show that interface-charge and strain co-mediated ME coupling can be clearly observed in the (001) Fe/BTO and the (001) LSMO/BTO structures. In particular, LSMO(001) films exhibit large transition thicknesses d_{tr}, indicating a more remarkable interface-charge mediated ME

effect. While in the (001) Ni/BTO and (0001) Co/BTO bilayers, the interface-charge mediated ME coupling may be relatively difficult to be observed explicitly, since the strain-mediated ME coupling is always dominant.

Acknowledgements

References

[1] R. Ramesh and N. A. Spaldin, Nat. Mater. **6**, 348 (2007).

[2] Y. Wang, J.-M. Hu, Y. H. Lin and C. W. Nan, NPG Asia Mater. **2**, 61 (2010).

[3] C. A. F. Vaz, J. Hoffman, C. H. Ahn, and R. Ramesh, Adv. Mater. **22**, 2900 (2010).

[4] C.-W. Nan, G. Liu, Y. Lin, and H. Chen, Phys. Rev. Lett. **94**, 197203 (2005).

[5] W. Eerenstein, N. D. Mathur, and J. F. Scott, Nature **442**, 759 (2006).

[6] M. Bibes and A. Barthélémy, Nat. Mater. **7**, 425 (2008).

[7] J.-M. Hu, Z. Li, J. Wang, and C. W. Nan, J. Appl. Phys. **107**, 093912 (2010).

[8] J.-M. Hu, Z. Li, J. Wang, J. Ma, Y. H. Lin, and C. W. Nan, J. Appl. Phys. **108**, 043909 (2010).

[9] J.-M. Hu, Z. Li, Y. H. Lin, and C. W. Nan, Phys. Status Solidi RRL **4**, 106 (2010).

[10] M. Liu, O. Obi, J. Lou, Y. J. Chen, Z. H. Cai, S. Stoute, M. Espanol, M. Lew, X. Situ, K. S. Ziemer, V. G. Harris, and N. X. Sun, Adv. Funct. Mater. **19**, 1826 (2009).

[11] M. Liu, O. Obi, Z. Cai, J. Lou, G. Yang, K. S. Ziemer, and N. X. Sun, J. Appl. Phys. **107**, 073916 (2010)

[12] C. Thiele, K. Dorr, O. Bilani, J. Rodel, and L. Schultz, Phys. Rev. B **75**, 054408 (2007).

[13] W. Eerenstein, M. Wiora, J. L. Prieto, J. F. Scott, and N. D. Mathur, Nat. Mater. **6**, 348 (2007).

[14] S. Sahoo, S. Polisetty, C.-G. Duan, S. S. Jaswal, E. Y. Tsymbal, and C. Binek, Phys. Rev. B **76**, 092108 (2007).

[15] J. J. Yang, Y. G. Zhao, H. F. Tian, L. B. Luo, H. Y. Zhang, Y. J. He, and H. S. Luo, Appl.

Phys. Lett. **94**, 212504 (2009).

[16] J. Lou, M. Liu, D. Reed, Y. H. Ren, and N. X. Sun, Adv. Mater. **21**, 4711 (2009).

[17] S. Geprags, A. Brandlmaier, M. Opel, R. Gross, and S. T. B. Goennenwein, Appl. Phys. Lett. **96**, 142509 (2010).

[18] J.-M. Hu and C. W. Nan, Phys. Rev. B **80**, 224416 (2009).

[19] H. J. A. Molegraaf, J. Hoffman, C. A. F. Vaz, S. Gariglio, D. van der Marel, C. H. Ahn, and J. M. Triscone, Adv. Mater. **21**, 3470 (2009).

[20] C. A. F. Vaz, J. Hoffman, Y. Segal, J. W. Reiner, R. D. Grober, Z. Zhang, C. H. Ahn, and F. J. Walker, Phys. Rev. Lett. **104**, 127202 (2010).

[21] M. Weisheit, Science **315**, 349 (2007).

[22] T. Maruyama, Y. Shiota, T. Nozaki, K. Ohta, N. Toda, M. Mizuguchi, A. A. Tulapurkar, T. Shinjo, M. Shiraishi, S. Mizukami, Y. Ando, and Y. Suzuki, Nat. Nanotech. **4**, 158 (2009).

[23] M. Endo, S. Kanai, S. Ikeda, F. Matsukura, and H. Ohno, Appl. Phys. Lett. **96**, 212503 (2010).

[24] P. Borisov, A. Hochstrat, X. Chen, W. Kleemann, and C. Binek, Phys. Rev. Lett. **94**, 117203 (2005).

[25] V. Laukhin, V. Skumryev, X. Martí, D. Hrabovsky, F. Sánchez, M. V. García-Cuenca, C. Ferrater, M. Varela, U. Lüders, J. F. Bobo, and J. Fontcuberta, Phys. Rev. Lett. **97**, 227201 (2006).

[26] Y. H. Chu, L. W. Martin, M. B. Holcomb, M. Gajek, S. J. Han, Q. He, N. Balke, C. H.

Yang, D. Lee, W. Hu, Q. Zhan, P. L. Yang, A. Fraile-Rodriguez, A. Scholl, S. X. Wang, and R. Ramesh, Nat. Mater. **7**, 478 (2008).

[27] H. Béa, M. Bibes, F. Ott, B. Dupé, X. H. Zhu, S. Petit, S. Fusil, C. Deranlot, K. Bouzehouane, and A. Barthélémy, Phys. Rev. Lett. **100**, 017204 (2008).

[28] D. Lebeugle, A. Mougin, M. Viret, D. Colson, and L. Ranno, Phys. Rev. Lett. **103**, 257601 (2009).

[29] D. Lebeugle, A. Mougin, M. Viret, D. Colson, J. Allibe, H. Béa, E. Jacquet, C. Deranlot, M. Bibes, and A. Barthélémy, Phys. Rev. B **81**, 134411 (2010).

[30] D. Peterka, A. Enders, G. Haas, and K. Kern, Phys. Rev. B **66**, 104411 (2002).

[31] J. X. Zhang, Y. L. Li, D. G. Schlom, L. Q. Chen, F. Zavaliche, R. Ramesh, and Q. X. Jia, Appl. Phys. Lett. **90**, 052909 (2007).

[32] J. Lou, R. E. Insignares, Z. Cai, K. S. Ziemer, M. Liu, and N. X. Sun, Appl. Phys. Lett. **91**, 182504 (2007).

[33] R. C. O' Handley, O. S. Song, and C. A. Ballentine, J. Appl. Phys. **74**, 6302 (1993).

[34] R. Vollmer, Th. Gutjahr-Löser, J. Kirschner, S. van Dijken, and B. Poelsema, Phys. Rev. B **60**, 6277 (1999).

[35] A. Stupakiewicz, A. Maziewski, K. Matlak, N. Spiridis, M. Slezak, T. Slezak, M. Zajac, and J. Korecki, Phys. Rev. Lett. **101**, 217202 (2008).

[36] The parameters used for numerical calculations are as follows. For Fe, $c_{11}=229$ GPa, $c_{12}=134$ GPa, $K_1=0.048$ MJ/m^3, $K_2=0.0001$ MJ/m^3, $B_1=-3.43$ MJ/m^3, $M_s=1.7\times10^6$ A/m (Ref. 18), $K_s=0.29$ mJ/m^2 (Ref. 22); for Ni, $c_{11}=246.5$ GPa, $c_{12}=147.3$ GPa, $K_1=-0.0045$

MJ/m^3, K_2=-0.0023 MJ/m^3, B_1=9.2 MJ/m^3, M_s=4.85×10^5 A/m (Ref. 18), K_s=-0.31 mJ/m^2 (Ref. 34); for La$_{0.88}$Sr$_{0.1}$MnO$_3$, c_{11}=200 GPa, c_{12}=105 GPa, K_1=0.127 MJ/m^3, K_2=-0.174 MJ/m^3, K_s=0.5 mJ/m^2, B_1=-1.43 MJ/m^3, M_s=3×10^5 A/m (Refs. 37–39); for hexagonal Co, c_{11}=307 GPa, c_{12}=165 GPa, c_{13}=103 GPa, c_{33}=358 GPa, c_{44}=75.5 Gpa, K_1=0.513 MJ/m^3, K_2=0.013 MJ/m^3, B_1=-8.1 MJ/m^3, B_2=-29 MJ/m^3, B_3=28.2 MJ/m^3, B_4=29.4 MJ/m^3, M_s=1.45×10^6 A/m (Ref. 40), K_s=1.16 mJ/m^2 (Ref. 35).

[37] Z.-H. Wang, H. Kronmüller, O. I. Lebedev, G. M. Gross, F. S. Razavi, H. U. Habermeier, and B. G. Shen, Phys. Rev. B **65**, 054411 (2002).

[38] Y. F. Popov, A. M. Kadomtseva, G. P. Vorob'ev, V. Y. Ivanov, A. A. Mukhin, A. K. Zvezdin, and A. M. Balbashov, J. Appl. Phys., **83**, 7160 (1998).

[39] J. O'Donnell, M. S. Rzchowski, J. N. Eckstein, and I. Bozovic, Appl. Phys. Lett. **72**, 1775 (1998).

[40] D. Sander, A. Enders, and J. Kirschner, J. Magn. Magn. Mater. **200**, 439 (1999).

[41] Y. Zhang, J. Liu, X. H. Xiao, T. C. Peng, C. Z. Jiang, Y. H. Lin, and C. W. Nan, J. Phys. D: Appl. Phys. **43**, 082002 (2010).

[42] C.-G. Duan, J. P. Velev, R. F. Sabirianov, Z. Zhu, J. Chu, S. S. Jaswal, and E. Y. Tsymbal, Phys. Rev. Lett. **101**, 137201 (2008).

[43] T. Y. Cai, S. Ju, J. Lee, N. Sai, A. A. Demkov, Q. Niu, Z. Li, J. Shi, and E. G. Wang, Phys. Rev. B **80**, 140415 (2009).

[44] C.-G. Duan, C.-W. Nan, S. S. Jaswal, and E. Y. Tsymbal, Phys. Rev. B **79**, 140403 (2009).

Figure Captions

FIG. 1. Electric voltage dependence of (a) the in-plane piezostrain ε_p generated in the (001) BaTiO$_3$ (BTO) film and (b) the surface anisotropy energy change ΔK_s in the Fe(001), Ni(001) and Co(0001) films.

FIG. 2. (a) Electric voltage-induced change of the H_{eff}^{OP}, i.e., ΔH_{eff}^{OP}, in the (001) Fe/BTO bilayers with various thicknesses d of the Fe(001) thin films. (b) Variation trends of ΔH_{eff}^{OP} as a function of the residual strain ε_0 in the (001) Fe/BTO bilayers at an applied voltage of 10 V.

FIG. 3. Variations of the out-of-plane effective anisotropy field, i.e., ΔH_{eff}^{OP}, with external electric voltages in (a) the (001) Ni/BTO and (b) the (0001) Co/BTO bilayers with different thicknesses d of the Ni or Co thin films.

FIG. 4. (a) Electric voltage dependence of the surface anisotropy energy change ΔK_s in the (001)-oriented La$_{0.88}$Sr$_{0.1}$MnO$_3$ (LSMO) film. Electric voltage-induced change of the H_{eff}^{OP}, i.e., ΔH_{eff}^{OP}, in the (001) LSMO/BTO bilayers with different thicknesses d of the LSMO thin films, at (b) T=300 K and (c) T=5 K.
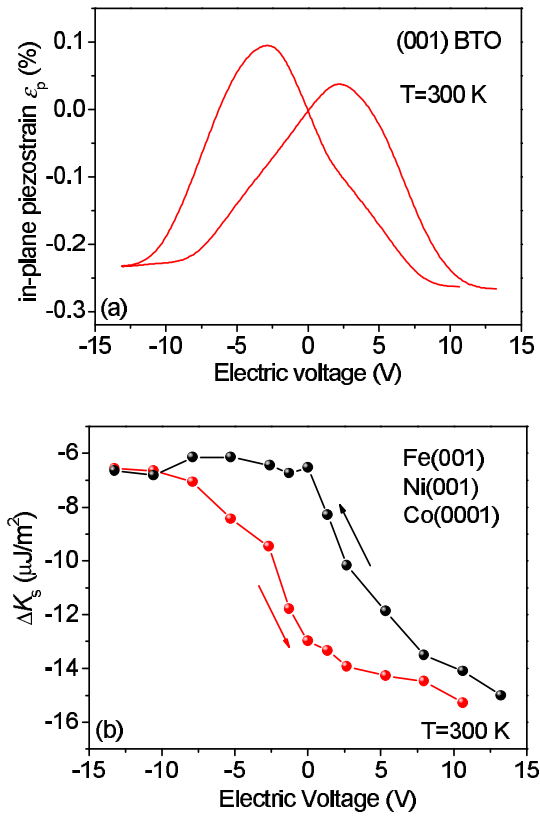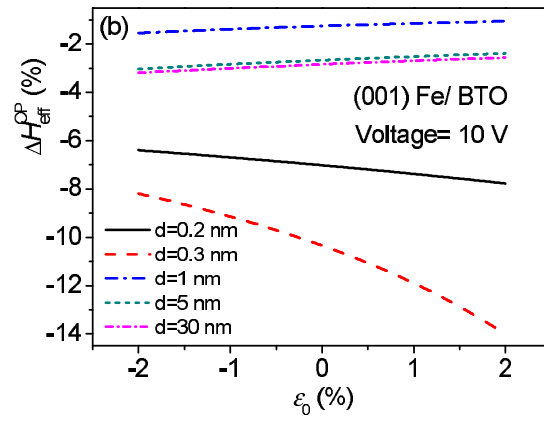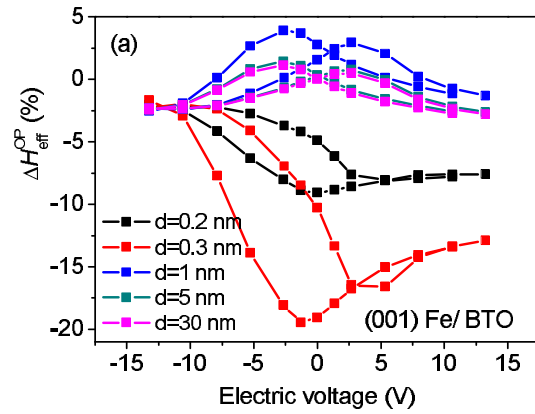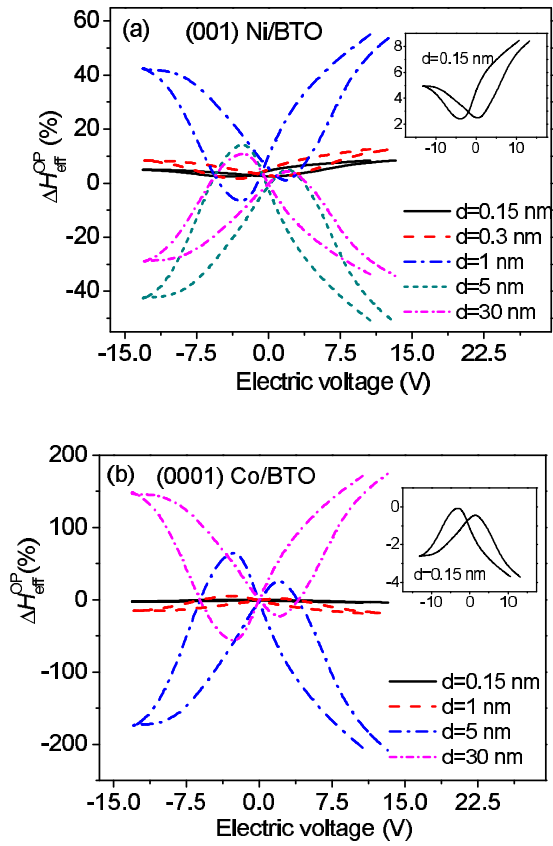
Figure 1   LY12454

Figure 1   LY12454   10JAN2011

Figure 2   LY12454

Figure 2   LY12454   10JAN2011

Figure 3   LY12454

Figure 3   LY12454   10JAN2011

Figure 4   LY12454

Figure 4   LY12454   10JAN2011